Cell division in walled Bacillus subtilis and cell wall-lacking Acholeplasma laidlawii

Gao, Y.

Publication date
2019

Document Version
Other version

License
Other

CHAPTER

6

Suppressing the growth defect of *ftsA* mutants

Yongqiang Gao

Leendert W. Hamoen

ABSTRACT

The conserved cell division protein FtsA acts as the primary membrane anchor for the key cell division protein, the tubulin homologue FtsZ. Its absence in *Bacillus subtilis* causes a division defect, resulting in longer cells, but it also slows down overall growth. The latter is not seen in cells depleted for FtsZ, suggesting that the growth phenotype is unrelated to cell division. To determine genetic factors involved in the reduced growth rate of *ftsA* deletion mutants, we performed a transposon mutagenesis. One of the best suppressor mutants found was a deletion of the *yczN-yczM* operon encoding a putative toxin pair. How this can be linked to the absence of FtsA remains unclear.

INTRODUCTION

Bacterial cell division is orchestrated by the tubulin homologue FtsZ, which polymerizes into a ring-like structure at midcell with the aid of the membrane anchor FtsA [1]. FtsA is widespread among bacteria and essential for cell division in *Escherichia coli* [2-4]. However, in *Bacillus subtilis*, deletion of *ftsA* does not prevent cell division. Nevertheless, such a mutant is filamentous, grows slower and has a sporulation defective [1,5]. The reason that *B. subtilis* can grow without FtsA is that this organism, like all Gram-positive bacteria, possesses an alternative membrane anchor for FtsZ polymers, the protein SepF [6].

Cytokinesis is initiated by polymerization of FtsZ into a ring-like structure at midcell, the Z-ring, which provides the scaffold for recruitment of the membrane localized late cell division proteins responsible for synthesis of the septal cell wall [7]. Cell division is considered an autonomous process, and depletion of FtsZ, although blocking cell division, does not prevent growth, resulting in exponentially expanding filamentous cells that will eventually lyse. In fact, transcriptome experiments of FtsZ depleted cells in both *B. subtilis* and *E. coli* showed only a minimal effect on global gene regulation [8,9]. However, the growth defect of an *ftsA* mutant suggests some link between cell division and other cellular process. To find out, we setup a new transposon selection system to find suppressors of the *ftsA* growth defect, and we found that removal of a putative toxin pair restores growth.

RESULTS & CONCLUSION

Slow growth of Δ*ftsA* mutant

B. subtilis ftsA deletion mutants have been reported to grow slower and they show a clear impaired cell division, resulting in elongated cells (Fig. 1). To confirm that the reduction in growth is not related to the cell division defect, we compared the growth rate with cells in which FtsZ was depleted. For this, we used a strain containing *ftsZ* under control of the IPTG-inducible *Pspac* promoter (strain GYQ572). Growth of this strain in the absence of IPTG resulted in very filamentous cells that eventually lysed, however the growth rate, measured as optical density, was comparable to the wild type strain (Fig. 1), confirming that the growth defect caused by the *ftsA* deletion is not related to cell division.

Suppressor mutagenesis

To determine why the absence of FtsA affects growth, we tried to find suppressor mutations. However, the reduced growth of an *ftsA* mutant under normal conditions was insufficient to select suppressors based on colony size. We tried to exacerbate the phenotype by growing cells under different stress conditions and found that Δ*ftsA* cells grow much slower compared to wild type cells on agar plates that contain 1 M of sodium chloride. This opened the way to screen for suppressor mutants.

Δ*ftsA* cells showed a reduced level of genetic competence and we were unable to directly transform plasmid pMarB, carrying the mariner transposable element TnYLB-1 [10], into this strain. Therefore we transformed wild type *B. subtilis* simultaneously with chromosomal DNA from strain GYQ300 containing a chloramphenicol selectable *ftsA* deletion (*ftsA*::*cmR*) and pMarB. A transformant containing both the plasmid and the *ftsA* mutation was grown at 50 °C, to activate the transposon and to lose the plasmid, and the culture was spread onto nutrient agar plates containing 1 M sodium chloride, resulting in approximately 75000 transposon colonies. The largest colonies were picked, and the growth rates were checked using microplate to ensure the mutants grew faster than the Δ*ftsA* strain.

Two rounds of backcrossing were performed to ensure that the transposon insertion was linked to faster growth.

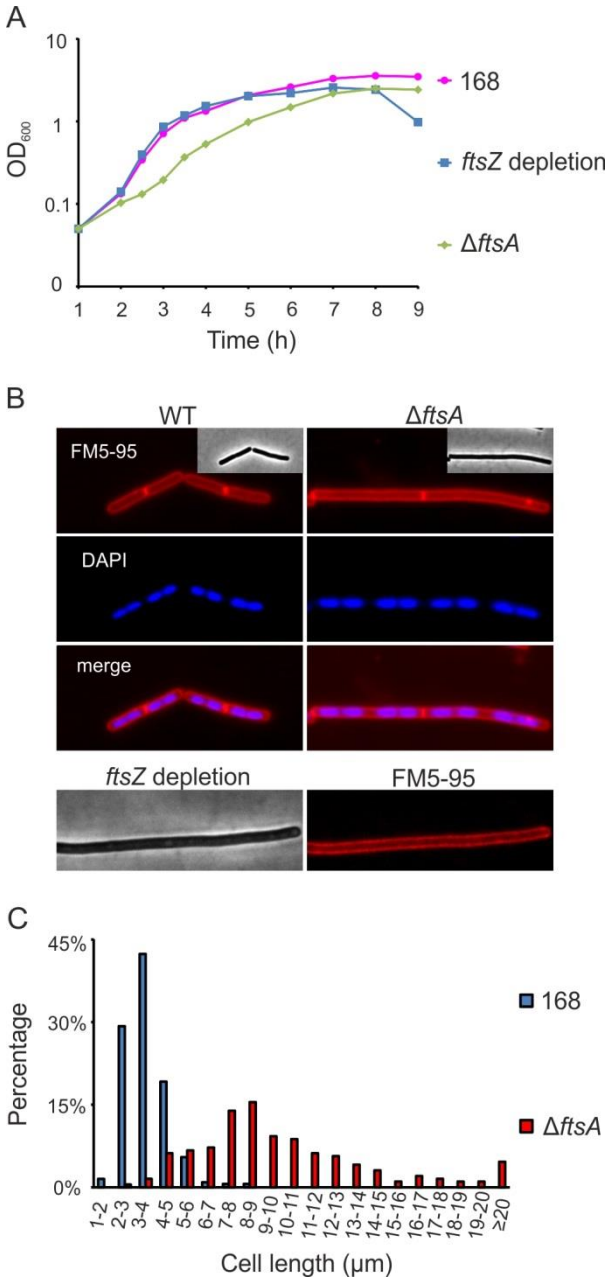

Fig. 1. Defect of growth and cell division caused by a *ftsA* deletion.

(A) Growth curve of 168, GYQ572 (*ftsZ::Pspac-ftsZ*) and GYQ300 (Δ*ftsA::cat*) grown in LB medium. (B) Microscopic images of 168 (*wt*), GYQ300 (Δ*ftsA*) and GYQ572 (*ftsZ::Pspac-ftsZ*) grown in LB medium without IPTG. Cell membrane and chromosomes are stained with FM5-95 and DAPI, respectively. Scale bar is 5 μm. (C) Histogram of cell length of 168 and GYQ300, collected at the log-phase in (A).

17 transposon mutants were selected for insertion analysis, and after sequencing, we found 8 suppressor mutants containing a transposon insertion in the unknown gene *yfhJ*, 7 mutants containing a transposon in the promoter region of the *yczN-yczM* operon, encoding putative type-I toxins [11,12], one mutant containing a transposon in *ydgG*, coding for a putative transcription factor [13], and another mutant containing a transposon insertion in *yfkA*, encoding a putative Fe-S oxidoreductase [14] (Fig. 2).

Conformation of suppressor phenotype

To confirm whether inactivation of the transposon targeted genes was indeed responsible for the increases growth rate, we replaced the complete genes by antibiotic markers. These markers were devoid of terminator sequences in order to reduce any downstream effects. *yfhJ, yczN* and *yczM* were replaced by a kanamycin resistance cassette, and *ydgG* and *yfkA* by an erythromycin resistance cassette. As shown in Fig. 3A, deletion of *yfhJ, yczN* and *yczM* improved the growth rate of a Δ*ftsA* mutant, and the complete deletion of the *yczN-yczM* operon showed even a better repression of the growth defect of Δ*ftsA*. The *ydgG* deletion did not improve the growth rate of Δ*ftsA* (Fig. 3B). However, this gene is the first in an operon, and when we deleted the downstream located gene *ydgH*, again the growth rate of a Δ*ftsA* mutant increased, indicating that the transposon insertion in *ydgG* was isolated because of a polar effect on *ydgH* expression. YdgH encodes a membrane transporter of unknown function. *yfkA* is the first gene in the *yfkA-yfkC* operon. However, only the *yfkA* deletion showed a slight improvement in the growth rate when introduced in a Δ*ftsA* mutant, whereas an *yfkC* deletion actually reduced the growth rate. Overall, the best suppressors of the Δ*ftsA* growth phenotype were the *yczN-yczM* and ydgH deletions, although none of them were able to completely restore the growth defect.

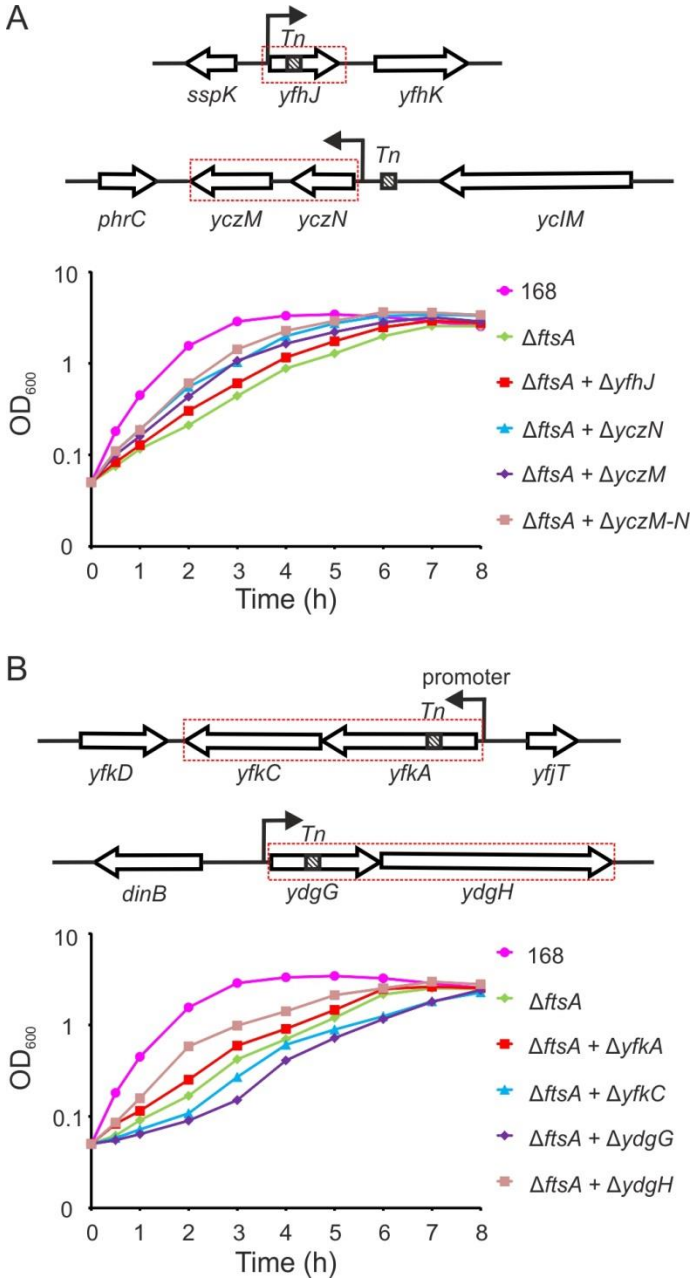

Fig. 2. Suppressors rescuing the growth defect of a Δ*ftsA* mutation

The screened transposon insertion sites on the chromosome of the strain GYQ300 (Δ*ftsA::cat*), and the relevant growth curve of strains 168, GYQ300, GYQ306 (Δ*ftsA::cat* Δ*yfhJ::Kan*), GYQ313 (Δ*ftsA::cat* Δ*yczN::Kan*), GYQ318 (Δ*ftsA::cat* Δ*yczM::Kan*), GYQ319 (Δ*ftsA::cat* Δ*yczN-M::Kan*), GYQ351 (Δ*ftsA::cat* Δ*yfkA::Kan*), GYQ352 (Δ*ftsA::cat* Δ*yfkC::Kan*), GYQ353 (Δ*ftsA::cat* Δ*ydgG::Kan*) and GYQ354 (Δ*ftsA::cat* Δ*ydgH::Kan*) grown in LB medium. The red dotted box indicates the relevant genes and operons.

Conclusion

Our transposon suppressor mutagenesis results suggest that part of the growth defect of an *ftsA* mutant is the activation of the *yczN-yczM* operon. The encoded proteins have been classified as paralogs of the YhzE family, which comprises type-I Toxin/Antitoxin systems [11]. These proteins have a conserved hydrophobic region and variable C-terminal and N-terminal domains. The N-terminus is always rich in glycines and aromatic residues. Normally, the antitoxin is a small antisense RNA adjacent to the toxin gene that base pairs with the toxin mRNA, preventing translation. However, no antisense RNA could be detected in the *yczN-yczM* operon based on previous transcriptome studies [11], and in fact we could not detect any expression of these genes in our transcriptome study either (thesis Chapter 5). It is therefore unclear why the *yczNM* deletion improves growth of a Δ*ftsA* mutant. The same is the case for the other transposon mutants. None of the targeted genes showed any relationship, suggesting that the growth retardation of an *ftsA* deletion is caused by pleiotropic effects.

MATERIALS AND METHODS

Bacterial strains and general methods

Strains used in this study are listed in Table. 1, *B. subtilis* and its derivatives were grown in LB medium supplemented with the appropriate antibiotics at the following concentrations: kanamycin 5 μg/ml, chloramphenicol 5 μg/ml, and erythromycin 2 μg/ml. *E. coli* Top10, used for plasmid construction and propagation, was cultivated in LB medium containing 100 μg/ml ampicillin. All above strains were cultivated at 37 °C while *E. coli* strains were at 30 °C. PCR, plasmid isolation and *E. coli* transformation were performed using standard methods. Gibson assembly cloning technology was applied for all the plasmid construction [15]. *B. subtilis* chromosome purification was carried out according to the method described by Venema *et al.* [16], and transformation of competence *B. subtilis* cells was accomplished based on the method of the optimized two-step starvation procedure [17,18].

To characterize the growth of different strains, the overnight culture were diluted 1:100 into fresh pre-warmed LB at 37 °C, until the OD_{600} reached 0.5-0.6 (log-phase), after which the culture were diluted into fresh pre-warmed LB medium again with the final OD_{600} of 0.05. Growth was followed at 37 °C by measuring the OD_{600} 0.5h or 1h intervals.

For *ftsZ* depletion, the overnight culture containing 0.5 mM IPTG, was diluted into fresh pre-warmed LB with 0.5 mM IPTG, and grew to the OD_{600} of 0.5-0.6. Spin down the culture with 7000 rpm for 1 min, and washed twice with pre-warmed LB. Afterwards, the washed cells were diluted into fresh pre-warmed LB without IPTG to the final OD_{600} of 0.05. The growth was monitored by OD_{600} measurement with the interval of 0.5h or 1h.

Transposon mutagenesis

Random transposon mutagenesis of a Δ*ftsA* mutant was performed using plasmid pMarB, carrying the mariner transposable element TnYLB-1, as described by Breton *et al.*[10]. Chromosomal DNA from strain GYQ300 (*ftsA::cat*) and plasmid pMarB were simultaneously transformed into competence cells of *B. subtilis* wild type strain 168, and spread on plate and

grown at 30 °C for about 20 hr. Several transformants that were both chloramphenicol and erythromycin resistant, were picked and grown overnight in LB at 30 °C, and diluted the next morning into LB medium and grown at 30 °C until the OD_{600} was 0.2-0.3, after which growth continued at 48 °C for 2h. Aliquots were frozen and stored at -80 °C. Several dilutions of each collected culture were spread on the plates with either erythromycin or kanamycin and incubate at 50 °C overnight. The replication origin of pMarB is inactive at high (> 30 °C) temperatures. The transposon is kan^R, whereas the plasmid contains an erm^R marker, enabling the assessment of transposon insertion efficiency. The transposon culture with the highest ratio of Kan^R/erm^R was chosen for further experiment. An aliquot was plated onto nutrient agar plates supplemented with kanamycin and 1M NaCl, and incubated at 50 °C overnight. Large colonies were selected and check whether they grew faster than strain GYQ300 using microtiter plates. Two rounds of backcrosses were performed, to ensure that the transposon was linked to the suppressor phenotype, as follows. Chromosomal DNA of selected colonies were transformed into competence cells of *B. subtilis* 168, and chromosomal DNA of the resulting transformants were again transformed into competence *B. subtilis* 168 cells. The resulting transformants were transformed with chromosomal DNA of Δ*ftsA* mutant GYQ300. Finally inverse PCR amplification and subsequent sequencing was performed to determine the transposon insertion sites.

Plasmid Construction

Primers used for plasmid construction are listed in Table. 2. To construct the plasmids used for *yfhJ, yczN, yczM, and yczN/yczM* knockouts, the plasmid backbone was derived from pUC19 with primers YQ56/YQ57, and the kanamycin resistance cassette was amplified using primers YQ131/YQ132 and plasmid pAPNC213 *Kan* as template. The upstream and downstream regions of *yfhJ*, were amplified with primer pairs YQ123/YQ124 and YQ125/YQ126, respectively, using genomic DNA of *B. subtilis* 168 as template. The 4 fragments were assembled resulting in pYQ17. The upstream regions of *yczN, yczM* and *yczN-M* were amplified using primer pairs YQ127/YQ128, YQ128/YQ161, and YQ128/YQ161,

respectively, and the downstream regions of *yczN, yczM* and *yczN-M* were amplified with primer pairs YQ129/YQ130, YQ162/YQ130, and YQ129/YQ130, respectively. These fragments, together with the plasmid backbone and kanamycin resistance cassette were assembled, generating plasmids pYQ19, pYQ26 and pYQ27, respectively. All constructs were checked by enzyme restriction and sequencing.

The mutants Δ*yfhJ*(GYQ305), Δ*yczN*(GYQ312), Δ*yczM*(GYQ316) and Δ*yczN-yczM*(GYQ317), were constructed by transforming the plasmids pYQ17, pYQ19, pYQ26 and pYQ27 into the competence cells of 168, respectively.

Fluorescence light microscopy

Overnight cultures were diluted in LB medium, supplemented with the relevant antibiotics and samples were taken at exponentially growth and mounted onto microscope slides coated with a 1.3% agarose patch. Images were captured with Nikon CoolSnap camera with a Zeiss Axiovert 200M epifluorescence microscope running MetaMorph software. For cell length measurement, cells were mixed with membrane dye FM5-95 (90 μg/ml), prior to microscopic examinations, and the ChainTracer, based on Image J plugin Object J, was applied for measurement of bacterial cell length [19]. For DNA staining, 2 μg/ml DAPI was added into culture after samples were prepared for the following microscopy.

REFERENCES

1 Jensen, S. O., Thompson, L. S. & Harry, E. J. Cell division in *Bacillus subtilis*: FtsZ and FtsA association is Z-ring independent, and FtsA is required for efficient midcell Z-ring assembly. *Journal of bacteriology* **187**, 6536-6544, doi:10.1128/JB.187.18.6536-6544.2005 (2005).

2 Busiek, K. K. & Margolin, W. Bacterial actin and tubulin homologs in cell growth and division. *Current Biology* **25**, R243-R254 (2015).

3 Lutkenhaus, J. & Donachie, W. Identification of the *ftsA* gene product. *Journal of bacteriology* **137**, 1088-1094 (1979).

4 Donachie, W. *et al.* Role of the *ftsA* gene product in control of *Escherichia coli* cell division. *Journal of bacteriology* **140**, 388-394 (1979).

5 Beall, B. & Lutkenhaus, J. Impaired cell division and sporulation of a *Bacillus subtilis* strain with the *ftsA* gene deleted. *Journal of bacteriology* **174**, 2398-2403 (1992).

6 Duman, R. *et al.* Structural and genetic analyses reveal the protein SepF as a new membrane anchor for the Z ring. *Proceedings of the National Academy of Sciences of the United States of America* **110**, E4601-4610, doi:10.1073/pnas.1313978110 (2013).

7 den Blaauwen, T., Hamoen, L. W. & Levin, P. A. The divisome at 25: the road ahead. *Current opinion in microbiology* **36**, 85-94 (2017).

8 Arjes, H. *et al.* Failsafe Mechanisms Couple Division and DNA Replication in Bacteria. *Current Biology Cb* **24**, 2149-2155 (2014).

9 Arends, S. J. R. & Weiss, D. S. Inhibiting cell division in *Escherichia coli* has little if any effect on gene expression. *Journal of bacteriology* **186**, 880-884 (2004).

10 Le Breton, Y., Mohapatra, N. P. & Haldenwang, W. *In vivo* random mutagenesis of *Bacillus subtilis* by use of TnYLB-1, a mariner-based transposon. *Applied and environmental microbiology* **72**, 327-333 (2006).

11 Durand, S., Jahn, N., Condon, C. & Brantl, S. Type I toxin-antitoxin systems in *Bacillus subtilis*. *RNA biology* **9**, 1491-1497, doi:10.4161/rna.22358 (2012).

12 Fozo, E. M. *et al.* Abundance of type I toxin-antitoxin systems in bacteria: searches for new candidates and discovery of novel families. *Nucleic Acids Res* **38**, 3743-3759, doi:10.1093/nar/gkq054 (2010).

13 Zhu, B. & Stülke, J. *Subti Wiki* in 2018: from genes and proteins to functional network annotation of the model organism *Bacillus subtilis*. *Nucleic acids research* **46**, D743-D748 (2017).

14 Witzky, A. *et al.* EF-P Posttranslational Modification Has Variable Impact on Polyproline Translation in *Bacillus subtilis*. *mBio* **9**, e00306-00318 (2018).

15 Gibson, D. G. *et al.* Enzymatic assembly of DNA molecules up to several hundred kilobases. *Nature methods* **6**, 343 (2009).

16 Venema, G., Pritchard, R. & Venema-Schröder, T. Fate of transforming deoxyribonucleic acid in *Bacillus subtilis*. *Journal of bacteriology* **89**, 1250-1255 (1965).

17 Anagnostopoulos, C. & Spizizen, J. Requirements for transformation in *Bacillus subtilis*. *Journal of bacteriology* **81**, 741 (1961).

18 Hamoen, L. W., Smits, W. K., Jong, A. d., Holsappel, S. & Kuipers, O. P. Improving the predictive value of the competence transcription factor (ComK) binding site in *Bacillus subtilis* using a genomic approach. *Nucleic acids research* **30**, 5517-5528 (2002).

19 Syvertsson, S., Vischer, N. O., Gao, Y. & Hamoen, L. W. When Phase Contrast Fails: ChainTracer and NucTracer, Two ImageJ Methods for Semi-Automated Single Cell Analysis Using Membrane or DNA Staining. *PloS one* **11**, e0151267, doi:10.1371/journal.pone.0151267 (2016).

Supplementary information

Table 1. Strains and plasmids used in this study

Antibiotic resistance genes were abbreviated as follows: *kan* (kanamycin), *cat* (chloramphenicol), *erm* (erythromycin), *bla* (ampicillin).

Strains	Relevant features or genotype	Construction or reference
B.Subtilis		
168	*trpC2*	[1]
YK1226	*ftsA::cat aprE::Kan Pspac-ftsA*	Laboratory stock
GYQ300	*ftsA::cat*	168 transformed with YK1226
GYQ572	*ftsZ::*(*Kan Pspac-ftsZ*)	Chapter 5
GYQ312	*yczN::Kan*	This study
GYQ313	*ftsA::cat yczN::Kan*	GYQ312 transformed with GYQ300
GYQ316	*yczM::Kan*	This study
GYQ318	*ftsA::cat yczM::Kan*	GYQ316 transformed with GYQ300
GYQ317	*yczN-M::Kan*	This study
GYQ319	*ftsA::cat yczN-M::Kan*	GYQ317 transformed with GYQ300
GYQ305	*yfhJ::Kan*	This study
GYQ306	*ftsA::cat yfhJ::Kan*	GYQ305 transformed with GYQ300
BKE07955	*yfkA::erm*	BGSC stock
GYQ335	*trpC2 yfkA::erm*	168 transformed with BKE07955
BKE07940	*yfkC::erm*	BGSC stock
GYQ336	*trpC2 yfkC::erm*	168 transformed with BKE07940
BKE05640	*ydgG::erm*	BGSC stock
GYQ337	*trpC2 ydgG::erm*	168 transformed with BKE05640
BKE05450	*ydgH::erm*	BGSC stock
GYQ338	*trpC2 ydgH::erm*	168 transformed with BKE05450
GYQ351	*ftsA::cat yfkA::erm*	GYQ335 transformed with GYQ300
GYQ352	*ftsA::cat yfkC::erm*	GYQ336 transformed with GYQ300
GYQ353	*ftsA::cat ydgG::erm*	GYQ337 transformed with GYQ300
GYQ354	*ftsA::cat ydgH::erm*	GYQ338 transformed with GYQ300
E.coli		
Top10		Laboratory stock
Plasmid	**Relevant features or genotype**	**Construction or reference**
pUC19	*bla,* P*lac*	[2]
pAPNC213 *Kan*	*bla, aprE3', Kan, lacI,* P*spac, aprE5'*	[3]
pMarB	*bla, erm* P*ctc Himar1 Kan* (TnYLB-1)	[4]
pYQ17	*bla, up-yfhJ-Kan-down-yfhJ*	This study
pYQ19	*bla, up-yczN-Kan-down-yczN*	This study
pYQ26	*bla, up-yczM-Kan-down-yczM*	This study
pYQ27	*bla, up-yczM-Kan-down-yczN*	This study

Table 2. Primers sequences used in this study

Name	Sequence (5'-3')
YQ124	CGGGGATCCTCTAGAGTCGACTCGGAGATGTCCTGAATTG
YQ123	CCGCAACTGTCCATACTCTGGTGTGCAGTCTCCTTTCTTCAG
YQ131	CAGAGTATGGACAGTTGCGGATG
YQ132	TGGTTTCAAAATCGGCTCCGT
YQ125	CGGAGCCGATTTTGAAACCAAAAAACCTGCCGTTAACGAC
YQ126	CAAGCTTGCATGCCTGCAGGGGACAATTAACGGGCCATCT
YQ56	CCTGCAGGCATGCAAGCTTGGCGT
YQ57	TCGACTCTAGAGGATCCCCGGGT
YQ128	CGGGGATCCTCTAGAGTCGAGCAGGAAACCTATAATGTGAGAATC
YQ127	CGGAGCCGATTTTGAAACCACTTCTAAGCTGCTGACCGTCTC
YQ129	CCGCAACTGTCCATACTCTGTTGGCAGGGATAATAGTGGACA
YQ130	CAAGCTTGCATGCCTGCAGGAAGGCGTCAAAGCGGAATA
YQ161	CGGAGCCGATTTTGAAACCATAATCTCCATGAAGGCGGCA
YQ162	CCGCAACTGTCCATACTCTGTGCACCTCCTTGCGAGATTG

REFERENCES

1 Kunst, F. *et al.* The complete genome sequence of the gram-positive bacterium *Bacillus subtilis*. *Nature* **390**, 249 (1997).

2 Yanisch-Peron, C., Vieira, J. & Messing, J. Improved M13 phage cloning vectors and host strains: nucleotide sequences of the M13mpl8 and pUC19 vectors. *Gene* **33**, 103-119 (1985).

3 Morimoto, T. *et al.* Six GTP-binding proteins of the Era/Obg family are essential for cell growth in *Bacillus subtilis*. *Microbiology* **148**, 3539-3552 (2002).

4 Le Breton, Y., Mohapatra, N. P. & Haldenwang, W. *In vivo* random mutagenesis of *Bacillus subtilis* by use of TnYLB-1, a mariner-based transposon. *Applied and environmental microbiology* **72**, 327-333 (2006).